



Sources and radiocarbon ages of aerosol organic carbon along the east coast of China and implications for atmospheric fossil carbon contributions to China marginal seas

Meng Yu^{a,b}, Zhigang Guo^c, Xuchen Wang^a, Timothy Ian Eglinton^d, Zineng Yuan^e, Lei Xing^a, Hailong Zhang^a, Meixun Zhao^{a,b,*}

^a Key Laboratory of Marine Chemistry Theory and Technology, Ministry of Education, Ocean University of China, Qingdao, China

^b Laboratory for Marine Ecology and Environmental Science, Qingdao National Laboratory for Marine Science and Technology, Qingdao, China

^c Shanghai Key Laboratory of Atmospheric Particle Pollution and Prevention, Department of Environmental Science and Engineering, Fudan University, Shanghai, China

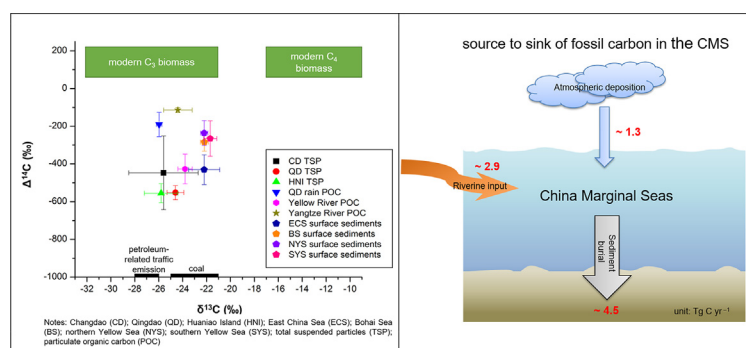
^d Geological Institute, Department of Earth Sciences, ETH Zürich, 8092 Zürich, Switzerland

^e Key Laboratory of Coastal Zone Environmental Processes and Ecological Remediation, Yantai Institute of Coastal Zone Research, Chinese Academy of Sciences, Yantai, China

HIGHLIGHTS

- ^{14}C and ^{13}C of aerosol samples from the east coast of China were analyzed.
- Fossil carbon was an important component of coastal aerosols.
- Strong seasonal variations of fossil carbon contribution were shown at Changdao.
- Atmospheric deposition is important for fossil carbon burial in the CMS.

GRAPHICAL ABSTRACT



ARTICLE INFO

Article history:

Received 29 August 2017

Received in revised form 27 October 2017

Accepted 17 November 2017

Available online xxx

Editor: Xuexi Tie

Keywords:

Aerosols

Radiocarbon (^{14}C) tracer

Total organic carbon

Fossil carbon

China marginal seas

ABSTRACT

Aerosol deposition is an important mechanism for the delivery of terrestrial organic carbon (OC) to marginal seas, but OC age characteristics of aerosols are not well constrained and their contributions to sediment OC burial have not been quantified. Total suspended particle samples were collected along the east coast of China at Changdao (CD), Qingdao (QD) and Huaniao Island (HNI), and were analyzed for total organic carbon (TOC) isotopes (^{13}C and ^{14}C) in order to bridge this information gap. TOC $\delta^{13}\text{C}$ and $\Delta^{14}\text{C}$ values ranged from -23.6 to -30.5% , and -153 to -687% , respectively, with the latter corresponding to ^{14}C ages ranging from 1280 to 9260 yr. Estimated contributions of fossil carbon to TOC based on ^{14}C mass balance approach ranged from 26 to 73%, with strong seasonal variations in fossil carbon observed at CD. Fossil carbon at CD showed the highest proportion (73%) in winter, reflecting anthropogenic emissions and the lowest proportion (26%) in summer, caused by biomass contribution (annual ave., $52\% \pm 17\%$). In contrast, the fossil carbon at both QD (57–64%) and HNI (57–67%) dominated throughout the year, reflecting local anthropogenic influences and long-range transport. Mass balance estimates indicate that atmospheric deposition and riverine export accounted for 31% and 69% of fossil carbon inputs to the China marginal seas (CMS) respectively, with fossil carbon burial efficiencies approaching 100% in the CMS. On a global scale, an atmospheric fossil carbon deposition flux of $17.2 \text{ Tg C yr}^{-1}$ was estimated, equivalent to 40% of the estimated fluvial flux to the ocean, and potentially accounting for 24–41% of fossil OC burial in

* Corresponding author at: Key Laboratory of Marine Chemistry Theory and Technology, Ministry of Education, Ocean University of China, No. 238, Songling Road, Qingdao, Shandong Province 266100, China.

E-mail address: maxzhao@ouc.edu.cn (M. Zhao).

marine sediments. Therefore, the atmospheric deposition constitutes an important source of fossil carbon to marine sediments, and could play a key role in regional and global scale OC budgets and biogeochemical cycles.

© 2017 Elsevier B.V. All rights reserved.

1. Introduction

Atmospheric transport represents a significant pathway for the transfer of natural and anthropogenic materials from land to oceans, augmenting riverine input. Atmospheric deposition of nutrients, trace metals and pollutants has influenced coastal and open ocean biogeochemical cycles (Duce et al., 1991; Mahowald, 2011). Aerosol deposition also plays a key role in the global carbon cycle (Jurado et al., 2008; Willey et al., 2000). A total of 58 Tg C yr⁻¹ of particulate organic carbon (POC) is delivered to the global ocean through dry and wet deposition (Jurado et al., 2008), equivalent to almost 30% of the annual river POC flux (~200 Tg C yr⁻¹) (Galy et al., 2015) and also to ~40% of total OC (TOC) burial (~160 Tg C yr⁻¹) in marine sediments (Burdige, 2005). Besides the riverine inputs, ¹⁴C data suggest that carbonaceous aerosols may also entrain a significant portion of pre-aged and fossil carbon (Heal, 2014; Matsumoto et al., 2001), and once buried in marine sediments, both carbon inputs may represent a long-term carbon sink. The transport and reburial of the non-modern carbon exerts minimal short-term influence on atmospheric CO₂ concentrations (Galy et al., 2008), however its mineralization – both in the terrestrial and marine environments – would result in an increase atmospheric CO₂. Therefore, it is important to constrain the different sources and fate of OC and their influence on atmospheric CO₂ and climate forcing on different time-scales. Fossil carbon may derive from natural weathering processes of continental rocks that is then transported oceanwards via riverine or atmospheric processes (Blair et al., 2003) or may be emitted as carbonaceous aerosols from fossil fuel combustion stemming from anthropogenic activities (Liu et al., 2013; Huang et al., 2014). Thus, increasing anthropogenic activity may enhance both the transport and burial of fossil carbon to the ocean.

Marginal seas are major loci of carbon sequestration, accounting for up to 90% of sediment OC burial in the global ocean (Hedges and Keil, 1995). The China marginal seas (CMS) in the western Pacific Ocean, including the Bohai Sea (BS), Yellow Sea (YS) and East China Sea (ECS), are important carbon sinks due to large-scale riverine and atmospheric inputs. With respect to the latter, the CMS are located in the downwind of the Asian continental outflow in spring and winter when the northerly wind prevails, during which atmospheric deposition of nutrients, heavy metals, toxic organic pollutants derived from anthropogenic activity could significantly influence marine ecosystems and biogeochemical processes (Shang et al., 2017; F. Wang et al., 2016; F.J. Wang et al., 2017). From a carbon cycle perspective, aerosol deposition has been also shown to be a significant source of carbon to the CMS, as indicated by studies of polycyclic aromatic hydrocarbons (PAHs, Lin et al., 2011; C. Wang et al., 2017) and black carbon (BC, Fang et al., 2015; Huang et al., 2016). For example, a study of BC budget in the BS suggested that contributions from atmospheric deposition were as important as those from riverine transport (Fang et al., 2015); and that atmospheric deposition contributed nearly 72% of PAHs to the CMS (C. Wang et al., 2017).

Natural abundance variations in radiocarbon (¹⁴C) provide a powerful diagnostic for distinguishing fossil and modern (biomass) carbon sources. ¹⁴C-based source apportionment studies have also indicated that fossil carbon can comprise an important fraction of BC and PAHs in carbonaceous aerosols and sediments (Hanke et al., 2017; Huang et al., 2016; Uchida et al., 2010). The deposition of fossil carbon may thus also influence marine ecosystems, biogeochemical processes and carbon cycling. However, previous OC budgets for CMS sediments have primarily focused on riverine inputs. For example, Wu et al. (2013) estimated that about 2 Tg C yr⁻¹ of fossil OC was buried in the

ECS inner shelf, exceeding annual inputs from the Yangtze River. Tao et al. (2016) estimated an unidentified contribution of 0.72 Tg C yr⁻¹ of pre-aged OC in the BS and YS. It could be inferred from both of the studies that atmospheric aerosols could serve as an important source of non-modern carbon to CMS sediments. Nevertheless, the importance of aerosol carbon contributions to the ocean carbon cycle remains poorly constrained. It is therefore necessary to characterize the fluxes and sources of aerosol OC in order to assess contributions to both regional and global ocean carbon budget.

In this study, aerosol total suspended particle (TSP) samples were collected along the east coast of China at Changdao (CD), Qingdao (QD) and Huaniao Island (HNI). There have been numerous prior studies on the composition, transport and deposition of major ions, trace elements and organic compounds in total suspended particulates and fine particulates at these sites (Feng et al., 2007, 2012; Guo et al., 2003; F. Wang et al., 2016), however, there has been no study of seasonal variations in ¹³C and ¹⁴C isotopic characteristics and no assessments of fossil carbon contributions to the CMS via atmospheric deposition. Hence, the main objectives of this study are to identify sources, to quantify radiocarbon ages of aerosol OC at these sites, and to estimate the contributions of aerosol-derived fossil carbon to the CMS sediment carbon budget.

2. Materials and methods

2.1. Study sites and sample collections

Aerosols were collected seasonally as total suspended particle (TSP) samples at CD, QD and HNI sites along the east coast of China (Fig. 1). Changdao (area, 56 km²) is near the demarcation line of the BS and YS and is located ~7 km north of the Shandong Peninsula, with limited local industrial activities. The sampling site at CD (37.90°N, 120.76°E, 90 m above sea level) was located on the rooftop of a radar station near the coast. Qingdao is a major coastal city situated in the southern tip of the Shandong Peninsula and the second largest city in Shandong province along the Yellow Sea coast with an urban population of ca. 4 million. The sampling site at QD (36.16°N, 120.50°E, 85 m above sea level) was on the rooftop of a building on the Ocean University of China campus. Huaniao Island (area, 3.28 km²) is located 66 km to the east of Shanghai coast, with 1000 inhabitants and no industrial activity. The sampling site of HNI (30.86°N, 122.67°E, 50 m above sea level) was located on the roof of a three-storey building, ~2 km from the population center. Thus, local anthropogenic inputs at CD and HNI are minor, while at QD local anthropogenic emissions may be substantial. All three sites are influenced by East Asian continental outflow toward to the Pacific Ocean, especially for CD and HNI since they have been classified as the background sites to monitor continental aerosol transport to the CMS (Feng et al., 2007; F.J. Wang et al., 2017).

Samples from CD and QD were collected on pre-combusted quartz filters (Whatman, QM-A, 20 × 25 cm²) by using a high volume sampler at a flow rate of 1 m³ min⁻¹ for 24 h. Samples from HNI were collected on quartz filters (Pall, 2500QAT, 20 × 25 cm²) at a flow rate of 0.3 m³ min⁻¹ for 23.5 h. All filters and aluminum foil were pre-combusted at 450 °C for 4 h to remove residual OC. After collection, filters were stored at –20 °C until analysis.

2.2. Carbon isotopic analysis

For TOC ¹³C and ¹⁴C analysis, freeze-dried samples were acidified by using 4 M HCl at room temperature to remove inorganic carbon and

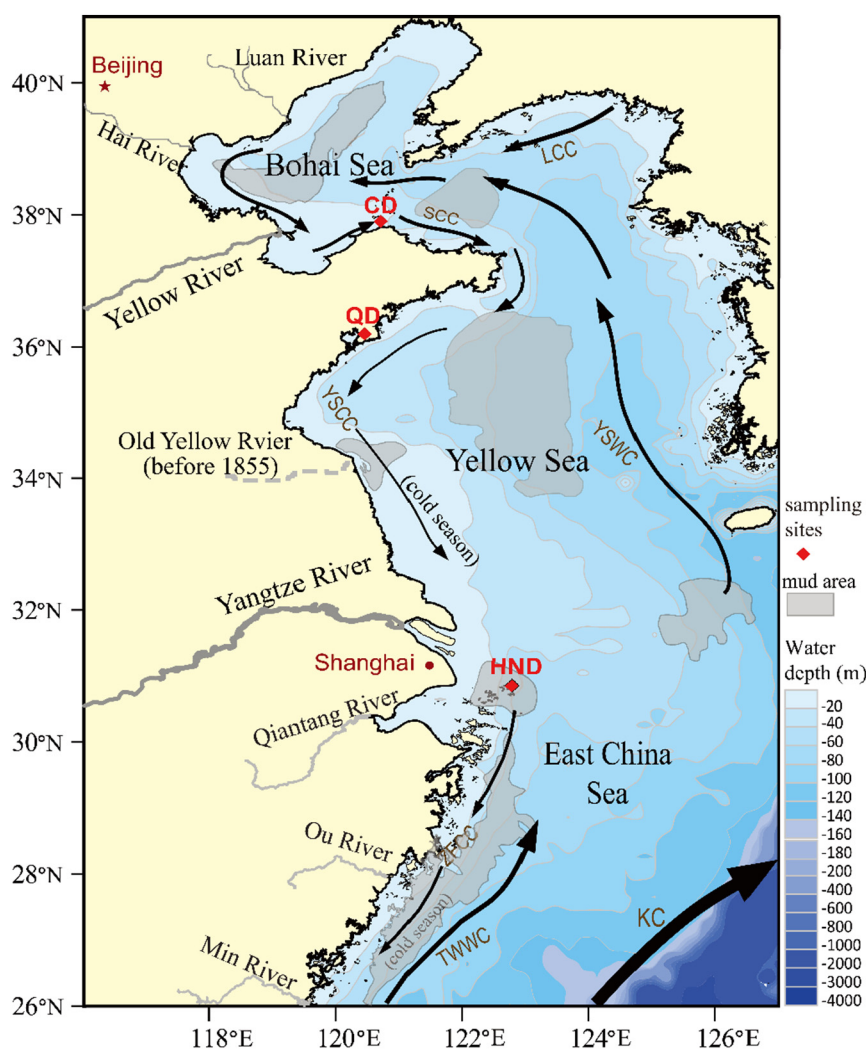


Fig. 1. The map of sampling sites (CD, QD and HNI) and adjacent CMS setting (modified from Hu et al., 2011). KC: Kuroshio Current; TWWC: Taiwan Warm Current; ZFCC: Zhejiang-Fujian Coastal Current; YSCC: Yellow Sea Coastal Current; YSWC: Yellow Sea Warm Current; SCC: Shandong Coast Current; LCC: Liaonan Coast Current.

then dried at 55 °C. The carbonate-free residues were combusted with CuO and Ag in evacuated, sealed quartz tubes at 850 °C for 2 h (Druffel et al., 1992; X. Wang et al., 2016). After cryogenic purification using isopropanol-dry ice mixture and liquid nitrogen, an aliquot of the purified CO₂ was analyzed for δ¹³C, while the remaining CO₂ was reduced to graphite for ¹⁴C measurement by accelerator mass spectrometry (AMS). All carbon isotopic measurements were carried out at the National Ocean Sciences Accelerator Mass Spectrometry (NOSAMS) facility at Woods Hole Oceanographic Institution (WHOI), USA. Radiocarbon results are reported as the fraction modern (Fm). The Δ¹⁴C (‰) values and corresponding un-calibrated ¹⁴C ages (years before present, yr B.P.) were calculated according to Stuiver and Polach (1977). The analytical precision for Δ¹⁴C measurements was 4–5‰ (McNichol et al., 2000). For CD and QD samples, an aliquot of filter was used for carbon isotope analyses; however for HNI, several samples collected in the same season were combined to get enough materials for ¹⁴C measurements.

3. Results

3.1. TOC and TSP concentrations

Table 1 lists properties of the TSP samples at the three sites. During the sampling period, TSP concentrations at the CD site ranged from 64.2 to 142.0 (avg. = 109.1 ± 29.8) μg/m³ with the highest value in

2012 autumn and the lowest value in 2014 summer. TOC concentrations ranged between 4.9 and 10.1 (avg. = 7.8 ± 2.0) μg/m³ with the highest value in 2014 winter. The TSP and TOC concentrations at the QD site ranged from 114.8 to 251.9 (avg. = 186.0 ± 56.3) μg/m³ and from 5.3 to 19.7 (avg. = 12.3 ± 5.9) μg/m³, respectively, with the highest values in 2014 winter and lowest values in 2014 summer. The TSP and TOC concentrations at HNI site ranged from 19.0 to 83.4 (avg. = 46.5 ± 29.0) μg/m³ and from 0.7 to 7.7 (avg. = 2.7 ± 2.8) μg/m³, respectively, with the highest values in 2012 winter and lowest values in 2014 summer. The TOC content (TOC%) values at these three sites exhibited a broadly similar range, with the highest value was found in winter for the QD and HNI sites, and in summer for the CD site. The mean TOC% value for CD, QD and HNI was 7.8 ± 3.2%, 6.3 ± 1.3% and 5.6 ± 2.7% respectively.

3.2. Carbon isotopic values (δ¹³C and Δ¹⁴C)

Temporal variations in the carbon isotopic composition (δ¹³C and Δ¹⁴C) of TOC differed between sites (Table 1). The δ¹³C values of CD displayed a wide range from −23.6 to −30.5‰ (avg. = −25.6 ± 2.9‰), with the lowest value in autumn. Δ¹⁴C values of CD samples also varied markedly, ranging from −153 to −687‰ (avg. = −447 ± 195‰), corresponding to ¹⁴C ages ranging from 1280 to 9260 yr (annual ave., 4700 ¹⁴C yr). Δ¹⁴C values also showed strong seasonal

Table 1
Results of TSP and TOC concentrations, TOC content; TOC $\delta^{13}\text{C}$, $\Delta^{14}\text{C}$, ^{14}C age; and f_f values.

Site	Sampling date	Season	TSP ($\mu\text{g}/\text{m}^3$)	TOC ^a ($\mu\text{g}/\text{m}^3$)	TOC (%)	$\delta^{13}\text{C}$ (‰)	$\Delta^{14}\text{C}$ (‰)	^{14}C age (yr)	f_f
Changdao	Oct. 23–24, 2012	AUT	142.0	4.9	3.5	−24.0	−490	5340	0.55 ± 0.04
	Jan. 9–10, 2014	WIN	100.7	10.1	10.0	−23.9	−687	9260	0.73 ± 0.03
	April 20–21, 2014	SPR	128.9	9.4	7.3	−23.6	−512	5700	0.57 ± 0.04
	Aug. 7–8, 2014	SUM	64.2	7.6	11.8	−25.9	−153	1280	0.26 ± 0.07
	Oct. 16–17, 2014	AUT	109.9	7.0	6.4	−30.5	−393	3950	0.47 ± 0.05
	Average		109.1	7.8	7.8	−25.6	−447	4700	0.52 ± 0.17
Qingdao	Jan. 2–3, 2014	WIN	251.9	19.7	7.8	−24.2	−590	7100	0.64 ± 0.03
	April 18–19, 2014	SPR	195.0	12.7	6.5	−25.3	−544	6240	0.60 ± 0.04
	Aug. 22–23, 2014	SUM	114.8	5.3	4.6	−25.1	−570	6720	0.62 ± 0.04
	Oct. 23–24, 2014	AUT	182.2	11.7	6.4	−23.9	−504	5570	0.57 ± 0.04
	Average		186.0	12.3	6.3	−24.6	−552	6390	0.61 ± 0.03
Huaniao Island	Jan., 2012	WIN	83.4	7.7	9.2	−24.4	−508	5640	0.57 ± 0.04
	Oct., 2012	AUT	28.3	1.7	6.1	−26.6	−518	5810	0.58 ± 0.04
	Jan., 2013	WIN	n.d. ^b	n.d. ^b	n.d. ^b	−25.1	−594	7180	0.64 ± 0.03
	April, 2013	SPR	55.3	1.9	3.4	−25.1	−621	7740	0.67 ± 0.03
	Aug., 2014	SUM	19.0	0.7	3.7	−27.8	−532	6040	0.59 ± 0.04
	Average		46.5	2.7	5.6	−25.8	−555	6440	0.61 ± 0.04

^a The TOC concentration and content were calculated by the resulting CO_2 from combustion. For HNI, several samples collected in the same season were combined to get enough materials for ^{14}C measurement.

^b n.d.: not determined because of one negative sample mass.

^c f_f : contribution of fossil carbon to the bulk OC

variations with lowest values (e.g., oldest ^{14}C ages) in winter and the highest values (youngest ages) in summer.

The $\delta^{13}\text{C}$ values of QD varied from −23.9 to −25.3‰ (avg. = −24.6 ± 0.7‰), with the highest value in autumn. The $\Delta^{14}\text{C}$ values of QD displayed a smaller range from −504 to −590‰ (avg. = −552 ± 37‰), with corresponding radiocarbon ages ranging from 5570 to 7100 yr (annual ave., 6390 ^{14}C yr). The oldest and youngest ^{14}C ages were found in winter and autumn respectively. The $\delta^{13}\text{C}$ values of HNI varied from −24.4 to −27.8‰ (avg. = −25.8 ± 1.4‰) with the lowest value in summer. The $\Delta^{14}\text{C}$ values of HNI ranged from −508 to −621‰ (avg. = −555 ± 50‰), with corresponding radiocarbon ages ranging from 5640 to 7740 yr (annual ave., 6440 ^{14}C yr). The oldest and youngest ^{14}C ages were found in 2013 spring and 2012 winter respectively. For the average $\delta^{13}\text{C}$ values, CD and HNI had comparable values which were lower than that of QD. For the average $\Delta^{14}\text{C}$ values, QD and HNI had comparable values which were lower than that of CD. QD samples showed smaller variations of both $\delta^{13}\text{C}$ and $\Delta^{14}\text{C}$ values than those of CD and HNI.

4. Discussion

4.1. Spatiotemporal variations of aerosol OC characteristics and sources

Previous studies showed that most air parcels at CD (Feng et al., 2007) and HNI (F. Wang et al., 2015) derived from the open sea in summer, but were transported from the northwest, driven by the East Asian monsoon, in winter. In spring and autumn, air parcels mostly emanated from the land with wind directions varying between northwest to north, and southeast or southwest to south (Feng et al., 2007; F. Wang et al., 2015). The backward trajectories in our sites were consistent with the wind direction during sampling period, as well as with previous studies which indicated that the atmosphere above these sites was impacted by regional environment and by continental outflow from northern China in spring, autumn and winter during our sampling periods (Figs. S1, S2, S3; Table S1). The CD and QD sites likely receive pollutants from major cities (e.g., Beijing and Tianjin) and from industries of the surrounding Bohai Economic Rim, and the HNI site may be strongly influenced by pollutants from cities and industries in the Yangtze River Delta (YRD) region, such as from Shanghai and continental outflow.

Winter and spring samples from our investigation collected during prevailing northwesterly winds (Figs. S1–S3) had higher TOC and TSP concentrations and lower $\Delta^{14}\text{C}$ values (Table 1), indicating emissions

from fossil fuel at all three sites. The higher $\delta^{13}\text{C}$ values in winter likely reflect contributions from coal burning (Fig. 3a), which has been suggested as the major trigger of air pollution in North China during the “heating season”. In addition, traffic emissions were also found to be one of the major causes of the heavy haze over China (Q. Wang et al., 2015). The slightly lower $\delta^{13}\text{C}$ values at HNI than those at CD and QD may reflect greater influence of traffic emissions in southern China compared with northern China. Previous studies also attributed the variation of $\delta^{13}\text{C}$ values of elemental carbon (EC) in Beijing and Shanghai during the wintertime to different types of energy consumption, with coal usage more important as a fossil carbon source in northern China (Chen et al., 2013). It was also interesting to note the increasing trend in $\Delta^{14}\text{C}$ values from CD to QD and then to HNI with higher TOC and TSP concentrations in QD and CD than HNI in winter, likely due to the higher proportional contributions from local fossil-fuel utilization in northern China. This trend suggests that air pollutants originating in northern China could be transported by the East Asian winter monsoon to southern China (F. Wang et al., 2016, Fig. S3).

$\Delta^{14}\text{C}$ values of summer samples from QD and HNI were comparably low to winter values, also indicating significant contributions from fossil fuel emissions. Furthermore, summer $\delta^{13}\text{C}$ values were generally lower than winter values, with seasonal differences ranging between 1.0 and 3.4‰. The winter and summer differences for $\delta^{13}\text{C}_{\text{OC}}$ and $\delta^{13}\text{C}_{\text{EC}}$ of $\text{PM}_{2.5}$ (aerodynamic diameter < 2.5 μm) in Chinese cities likely reflect variable fossil carbon sources, for example greater coal combustion during winter may result in higher $\delta^{13}\text{C}$ values while increasing petroleum-related traffic emissions in summer induce lower $\delta^{13}\text{C}$ values (Cao et al., 2011, Fig. 3a). These seasonal $\delta^{13}\text{C}$ differences were particularly evident at HNI when air parcels derive mostly from the ocean. Although located 66 km from the mainland coast, HNI may also be influenced by ship emissions from YRD port cluster (Fan et al., 2016; F. Wang et al., 2016). In contrast, CD exhibited the highest $\Delta^{14}\text{C}$ value in summer compared with values for other seasons and other sites, indicating a greater contribution from non-fossil sources. Although traffic emissions may still have contributed some OC to aerosols, as suggested by the distribution patterns of hopanes (Feng et al., 2007), this higher $\Delta^{14}\text{C}$ value together with the lowest TSP concentration in summer likely reflects clean air parcels emanating from the ocean (Fig. S1) that diluted anthropogenic pollutants or/and regional vegetation emissions. It is also worth noting that the most depleted $\delta^{13}\text{C}$ value (−30.5‰) occurred in 2014 autumn at CD. Compared with 2012 autumn sample, the 2014 autumn sample had both a lower $\delta^{13}\text{C}$ value and a higher $\Delta^{14}\text{C}$ value, likely reflecting OC inputs from C_3 plants, as also indicated by highest plant

wax contributions in autumn (Feng et al., 2007) or regional biomass burning of wood or agricultural waste (Zhang et al., 2017) in autumn.

Our study revealed significantly lower $\Delta^{14}\text{C}$ values for aerosol OC in comparison with modern atmospheric CO_2 values (Levin et al., 2003), suggesting that the fossil carbon from anthropogenic activity contributes an important fraction of OC to carbonaceous aerosols over the east China coast. A simple isotopic mass balance equation based on $\Delta^{14}\text{C}$ was applied to quantify the contributions of modern biomass sources (f_{bio}) and fossil carbon ($f_f = 1 - f_{\text{bio}}$) to the bulk OC in TSP samples (Gustafsson et al., 2009; Mandalakis et al., 2005; Sheesley et al., 2012; Zencak et al., 2007).

$$^{14}\text{C}_{\text{sample}} = ^{14}\text{C}_{\text{biomass}} \times f_{\text{bio}} + ^{14}\text{C}_{\text{fossil}} \times (1 - f_{\text{bio}})$$

The end member for fossil carbon $\Delta^{14}\text{C}_{\text{fossil}}$ is -1000‰ . For modern biomass, the end member $\Delta^{14}\text{C}_{\text{biomass}}$ is assumed to be between $+70$ and $+225\text{‰}$, which corresponds to contemporary CO_2 (Levin et al., 2003) and modern biomass combustion (Klinedinst and Currie, 1999). These modern biomass end members serve as upper and lower limits for the f_{bio} , which in turn determine the corresponding lower and upper limits for the f_f (Table 1). Results indicate that fossil carbon contributed 26–73% to the bulk OC at the three coastal sites (Fig. 2). The fossil carbon contribution at CD exhibited large seasonal variations with the highest proportions in winter (73%) and the lowest in summer (26%), with an annual average of $52 \pm 17\%$. In contrast, the fossil carbon contributions at QD and HNI displayed smaller seasonal variations, ranging from 57 to 64% (avg. = $61 \pm 3\%$) and from 57 to 67% (avg. = $61 \pm 4\%$), respectively, both indicating a dominant contribution of fossil sources to bulk OC throughout the year.

The highest fossil carbon contribution was found in winter at CD, and was possibly impacted by intense coal combustion activities from the Bohai Rim and northwestern China during the winter heating season. The lowest fossil carbon contribution in summer at CD may reflect arrival of clean air parcels (Fig. S1) or/and biogenic emissions from widespread growth of vegetation. In contrast to the large seasonal variation at the CD site, the constancy in fossil carbon contribution at the QD and HNI sites indicates a dominance of fossil sources throughout the year. Corresponding $\delta^{13}\text{C}$ values at HNI suggest a stronger influence of traffic emissions in summer than those in other northern cities. HNI is a relatively remote site, but receives higher anthropogenic inputs in spring and winter than that in summer under the influence of East Asian monsoon (Shang et al., 2017; F. Wang et al., 2016). An extremely persistent and severe haze event occurred in China in January 2013 caused by a combination of anthropogenic emissions and unusual atmospheric circulation (Fu and Chen, 2017; Huang et al., 2014). This coincides with the higher fossil carbon contribution (64–67%) in January and April 2013 at HNI site. The wind direction in summer is mostly from the sea at HNI (Fig. S3), yet fossil carbon contributions in summer were comparable with those in winter. This suggests that fossil carbon likely reflects regional emissions (e.g., from ship emissions) rather than from the long-range land transport. A model study in the YRD and ECS estimated that 85% of ship emissions occurred within 200 km of the coastline, potentially influencing the whole YRD region and greater eastern China (Fan et al., 2016). HNI is located 66 km to the east of the Shanghai coast and adjacent to the major shipping routes in the ECS, and it was under the impact of ship emissions transported from both the YRD and Yangshan port (one of the largest ports in the world). A previous study also found that ship emissions contributed significantly to HNI aerosols in summer (F. Wang et al., 2016), consistent with the high fossil carbon contribution observed in this study. The $\delta^{13}\text{C}$ and $\Delta^{14}\text{C}$ values at QD implied relatively constant fossil carbon sources, suggesting the persistent influence of anthropogenic activities. The Qingdao rainwater particulate samples collected during May to July 2014 were more enriched in ^{14}C than POC in airborne TSP samples (Fig. 3b), suggesting the importance of non-fossil OC in rainwater particulate

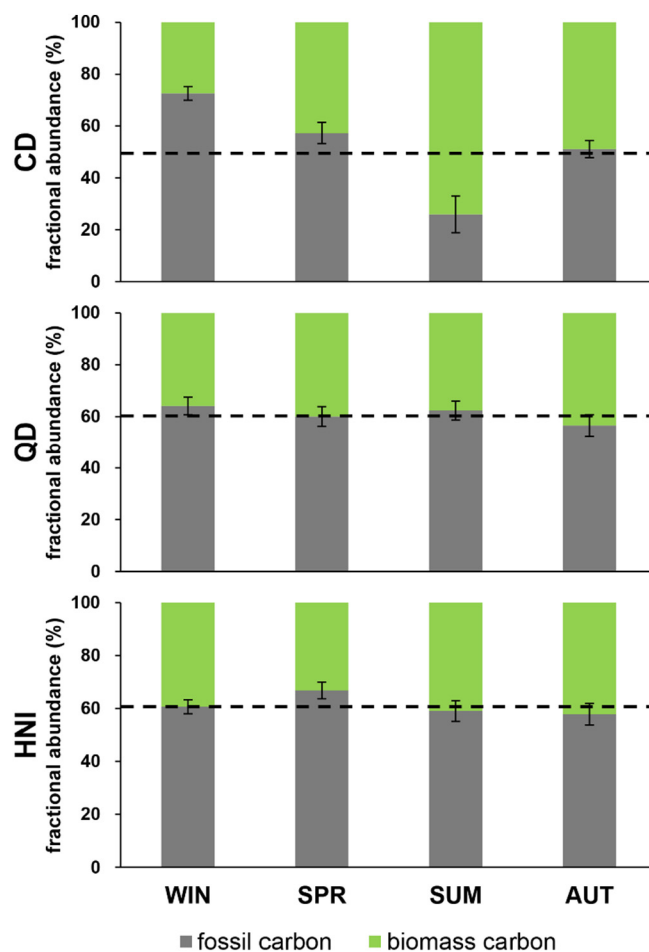


Fig. 2. Contributions of fossil and modern biomass carbon to bulk OC at CD, QD and HNI (the average value is plotted if two or more samples were collected). The dashed line represents the average contribution of fossil carbon to the bulk OC.

matter (X. Wang et al., 2016). This is consistent with observations at sites of Portugal and Switzerland (Zhang et al., 2015a) and implies that wet deposition in summer may preferentially scavenge the non-fossil OC, resulting in a corresponding increase in the proportion of fossil carbon in aerosols.

Average fossil carbon contributions to bulk OC observed in this study (ranging from 52 to 61%) were higher than that of total carbon (TC) at some rural or background sites (Zhang et al., 2014). For example, radiocarbon measurements on different carbon fractions in $\text{PM}_{2.5}$ samples at a regional background site on Hainan Island (southern China) revealed a dominance of non-fossil emissions, with fossil source contributions of only 23%, 38% and 19% to TC, EC and OC respectively (Zhang et al., 2014). On the other hand, these values were broadly similar with or slightly lower than those from sites impacted by heavy anthropogenic fossil-fuel emissions. For example, fossil carbon contribution was 61–65% at Yufa (Beijing, northern China) (Sun et al., 2012), 51% at Lhasa (Tibet, southwestern China) (Huang et al., 2010), 60% and 56% at Beijing and Shanghai during winter haze days (Zhang et al., 2015b). At Ningbo, the fossil carbon contribution to EC was 88% in winter and 60% in summer. This seasonal pattern was attributed to fossil fuel emissions from central and northern China transported by northwest winds in winter, and a greater contribution from biomass burning activities in southern and eastern China in summer (Liu et al., 2013). In contrast, at an urban site in Lhasa city, ^{14}C analysis of TC revealed a pattern of higher fossil carbon contribution (56%) in summer and autumn due to the traffic emissions during tourism season, and the lowest fossil carbon contribution (43%) in winter due to local wood burning (Huang et al., 2010).

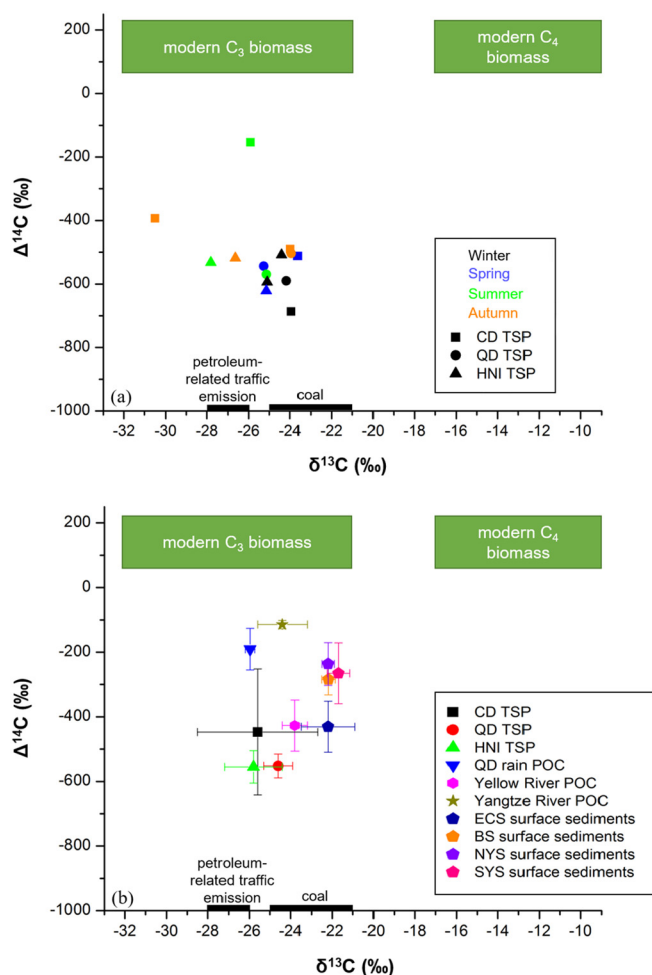


Fig. 3. Cross-plot of organic carbon $\delta^{13}\text{C}$ values versus $\Delta^{14}\text{C}$ values of (a) seasonal aerosol TSP samples at CD (square), QD (circle) and HNI (triangle) sites (different colors represent different seasons); (b) average TSP samples in this study and comparison with other published typical riverine and CMS sediment samples, including lower Yellow River POC (Tao et al., 2015; Wang et al., 2012; Xue et al., 2017); Yangtze River POC (Wang et al., 2012); QD rain POC from wet deposition (X. Wang et al., 2016); ECS surface sediments (Wu et al., 2013); BS, northern YS (NYS) and southern Yellow Sea (SYS) surface sediments (Bao et al., 2016; Xing et al., 2014, 2016). The end-member of modern biomass (C_3 and C_4 plants, upper green field) and fossil carbon (coal combustion and traffic emission like motor vehicle exhaust, lower thick black line) sources are also shown (Cao et al., 2011; Gustafsson et al., 2009; Lamb et al., 2006). (For interpretation of the references to color in this figure legend, the reader is referred to the web version of this article.)

In summary, fossil carbon contribution in winter at sites CD, QD and HNI was mainly influenced by local fossil fuel combustion and by the continental outflow. However, during summer season, site CD was strongly influenced by marine aerosols and biogenic emissions, while site HNI may be impacted by ship emissions from the YRD port cluster and site QD was mainly influenced by local fossil carbon emissions and inland source. Therefore at these coastal sites, local activities serve as the main sources of aerosol OC, augmented by inputs from long-range transport.

4.2. Implications for fossil carbon contributions to China marginal seas

The CMS system has been recognized a significant sink for different form of carbon, including TOC (Deng et al., 2006; Hu et al., 2016), pre-aged and fossil OC (Tao et al., 2016), BC (Fang et al., 2015; Huang et al., 2016), and PAHs (C. Wang et al., 2017). Regional budgets developed for BC and PAHs suggest that atmospheric deposition could be a significant source of OC to the CMS in addition to riverine inputs (Fang et al., 2015; C. Wang et al., 2017). Similarly, recent constraints on fossil carbon

delivery by the Yellow River and Yangtze River, and its burial in CMS (Hu et al., 2015; Tao et al., 2015, 2016; Wang et al., 2012; Wu et al., 2013; Xue et al., 2017) have indicated that aerosol deposition could be an important source for the both pre-aged and fossil carbon in the CMS. While detailed quantitative information is still lacking on aerosol fossil carbon fluxes to the CMS, the isotope characteristics of river POC, sedimentary TOC and aerosol OC can shed some light on this question. As shown in Fig. 3b, POC transported by Yellow River is more depleted in ^{13}C and ^{14}C than that of sedimentary OC in adjacent BS and YS. Assuming the Yellow River represents the dominant source of terrestrial OC to BS and YS, the addition of marine OC could explain the higher $\delta^{13}\text{C}$ and $\Delta^{14}\text{C}$ values of sedimentary OC. In contrast, POC transported by Yangtze River is more enriched in ^{14}C than adjacent ECS sedimentary OC, suggesting additional sources of OC to the ECS with older ^{14}C ages than that of the Yangtze River POC. The average age of aerosol OC at the three sites investigated in the present study was older than those of sedimentary OC in the CMS, indicating that atmospheric deposition may comprise an additional terrestrial source of old carbon to CMS besides the riverine input. Alternatively, OC aging may occur during transport processes (Bao et al., 2016) that could result in more ^{14}C -depleted TOC in ECS sediments. In order to further assess aerosol fossil carbon contributions to the CMS sedimentary OC we compare fossil OC fluxes associated with atmospheric deposition and riverine input with those of sedimentary burial.

Generally, the bulk carbonaceous aerosols (TC) are considered to include two sub-fractions - namely OC and EC (also termed BC). We assume that the TOC measured in our study is equivalent to the TC reported in the literature. We then estimate the atmospheric deposition flux of fossil carbon to CMS by using reported BC deposition data (Table 2) under the following assumptions. The average OC/BC ratio of 4.0 (Cao et al., 2007) is used to convert the reported atmospheric BC flux to TOC flux. A wet/dry deposition ratio of 2.2 for the Bohai Rim (Fang et al., 2015) is then used to estimate the wet and dry deposition of TOC flux to CMS. By multiplying the corresponding average f_f values of aerosol TSP, we then derive an estimated aerosol fossil carbon flux. As shown in Table 2, the average f_f value (0.56) of dry deposition from CD and QD was used for BS and YS estimates, and HNI result ($f_f = 0.61$) was used for ECS estimates. The average f_f value (0.58) of the three sites examined in this study was used for global-scale estimates. The average f_f value (0.23) of wet deposition was from QD rain POC samples (X. Wang et al., 2016). Therefore, based on the estimated atmospheric deposition of BC flux ($0.093 \text{ Tg C yr}^{-1}$) and wet/dry deposition ratio in BS (Fang et al., 2015), the dry and wet deposition of TOC flux is estimated at 0.15 and $0.32 \text{ Tg C yr}^{-1}$, respectively. By assuming the YS (area, $380,000 \text{ km}^2$) had the similar atmospheric deposition conditions per unit area to BS (area, $77,000 \text{ km}^2$), we determine an overall dry and wet deposition of TOC flux to the combined BS and YS was 0.86 and $1.90 \text{ Tg C yr}^{-1}$, respectively, and total fossil carbon deposition for the BS and YS of $0.92 \text{ Tg C yr}^{-1}$. Similarly, based on the estimated dry deposition flux of BC ($0.067 \text{ Tg C yr}^{-1}$) in ECS (Huang et al., 2016), dry and wet deposition of TOC flux was estimated to be 0.34 and $0.74 \text{ Tg C yr}^{-1}$, respectively, and atmospheric deposition of fossil carbon to the ECS was $0.38 \text{ Tg C yr}^{-1}$. Thus, the total aerosol fossil carbon deposition to the CMS is estimated at $1.30 \text{ Tg C yr}^{-1}$.

For the perspective of sources of terrestrial sediment to the eastern CMS, the Yellow River and Yangtze River are the dominant contributors (>66%) on a 100-year timescale (Zhou et al., 2014). Thus, for this preliminary estimation of fossil carbon inputs, we draw comparisons between atmospheric deposition and inputs from these two rivers for the eastern CMS, and exclude contributions from small rivers and coastal erosion. According to the long-term average POC flux of $3.44 \text{ Tg C yr}^{-1}$ (Tao et al., 2016) and f_f (0.41 ± 0.15) of Yellow River POC (Hu et al., 2015), a fossil OC flux of $1.41 \text{ Tg C yr}^{-1}$ is estimated to be discharged to the BS, with a significant portion being transported to the YS and possibly the ECS. Similarly, based on a TOC burial flux of 5.6 Tg C yr^{-1} in the BS and YS (Hu et al., 2016) and f_f (0.26 ± 0.05) in

Table 2Fossil carbon flux (Tg C yr^{-1}) of atmospheric deposition, riverine input and burial in the BS and YS, ECS and global ocean.

Region		TOC flux	f_f	Fossil carbon flux
BS and YS	Dry deposition	0.86 ^d	0.56	0.48
	Wet deposition	1.90 ^a	0.23 ^b	0.44
ECS	Atmospheric deposition	2.76		0.92
	Yellow River	3.44 ^c	0.41 ^d	1.41
	Sediment burial	5.6 ^e	0.26 ^f	1.46
	Dry deposition	0.34 ^g	0.61	0.21
	Wet deposition	0.74 ^g	0.23 ^a	0.17
	Atmospheric deposition	1.08		0.38
Global Ocean	Yangtze River	4.5 ^h	0.27–0.34 ^h	1.5 ^h
	Sediment burial	7.4	0.35–0.45 ^h	3.0
	(inner shelf, 5.0) ⁱ			(inner shelf, 2.0) ^h
	Dry deposition	11 ^j	0.58	6.4
Global Ocean	Wet deposition	47 ^j	0.23 ^b	10.8
	Atmospheric deposition	58 ^j		17.2
	Riverine input	200 ^k	0.20 ^k	43 ^k
	Sediment burial	160 ^l	0.26–0.45 ^{lh}	42–72

^a According to Fang et al. (2015) and assumed average OC/BC ratio was 4.0 (Cao et al., 2007).

^b According to X. Wang et al. (2016).

^c According to Tao et al. (2016).

^d According to Hu et al. (2015).

^e According to Hu et al. (2016).

^f According to Yoon et al. (2016).

^g According to Huang et al. (2016) and assumed average OC/BC ratio was 4.0 (Cao et al., 2007).

^h According to Wu et al. (2013).

ⁱ According to Deng et al. (2006).

^j According to Jurado et al. (2008).

^k According to Galy et al. (2015).

^l According to Burdige (2005).

the YS (Yoon et al., 2016), a corresponding fossil OC burial flux of $1.46 \text{ Tg C yr}^{-1}$ is estimated for the BS and YS. Combined with the fossil carbon flux delivered by the Yangtze River (1.5 Tg C yr^{-1}), this results in a total fossil carbon input to the CMS from fluvial and atmospheric sources of 4.2 Tg C yr^{-1} . Thus, the riverine input and atmospheric deposition accounted for 69% and 31% of the total input, respectively. These estimates contrast with the reported PAH budget which indicated that 72% of the total PAHs was from atmospheric deposition (C. Wang et al., 2017). While these contrasting fluxes imply different sources and transport pathways depending on carbon type, they nevertheless highlight the importance of atmospheric deposition as a vector for delivering fossil carbon to the CMS. The fossil carbon burial in CMS was 4.5 Tg C yr^{-1} slightly exceeds inputs. These preliminary estimates suggest highly efficient (approaching 100%) burial of fossil carbon in CMS sediments. Although we did not take into account inputs from other rivers or from coastal erosion processes, these preliminary estimates nevertheless imply that continental shelf sediments serve as a key sink key sink of fossil carbon, consistent with prior findings for BC in the BS and PAHs in eastern CMS (Fang et al., 2015; C. Wang et al., 2017).

In the BS and YS, atmospheric deposition corresponds to almost 65% of the Yellow River input of fossil OC. This percentage was comparable with results for black carbon in the BS (Fang et al., 2015), but differs to those for PAHs. C. Wang et al. (2017) found that atmospheric deposition of PAHs was nearly 13 times larger than the Yellow River input, and was similar to the burial flux in the BS and YS. In comparison for sediment fossil carbon, the estimates suggest that ~63% of the combined fossil carbon input ($2.33 \text{ Tg C yr}^{-1}$) from the Yellow River and atmospheric deposition was buried, with the remainder likely translocated or re-oxidized. This is broadly consistent with the fossil carbon budget estimated by Tao et al. (2016), who found that 70% of fossil carbon input was buried, even without considering atmospheric deposition. In contrast for the ECS, atmospheric deposition of fossil carbon ($0.38 \text{ Tg C yr}^{-1}$) is equivalent to only 25% of Yangtze River input, but may partly explain

the imbalance in fossil carbon fluxes between the Yangtze River input ($\sim 1.5 \text{ Tg C yr}^{-1}$) and the sedimentary burial on the inner shelf ($\sim 2 \text{ Tg C yr}^{-1}$) (Wu et al., 2013). However for the whole ECS shelf, additional sources of fossil carbon are required to reconcile the budget, with one plausible source being ocean current-driven transport of materials derived from Taiwanese rivers or from the BS and YS. Compared with ECS, the atmospheric deposition in the YS is likely overestimated given the assumption of uniform atmospheric deposition fluxes per unit area over the entire BS and YS, yielding higher proportions from atmospheric deposition of OC in comparison with riverine inputs to the BS and YS.

On a global scale, atmospheric deposition of TOC to the ocean through dry and wet deposition has been estimated at 11 Tg C yr^{-1} and 47 Tg C yr^{-1} (Jurado et al., 2008), equivalent to 29% of the riverine OC inputs. However, global atmospheric fossil carbon deposition to the ocean was estimated to be $17.2 \text{ Tg C yr}^{-1}$, corresponding to 40% of the riverine inputs (Table 2). Using the f_f value (0.26–0.45) in CMS sedimentary TOC and using a global OC burial flux in marine sediment of 160 Tg C yr^{-1} (Burdige, 2005), we estimate a global ocean fossil OC burial flux of 42 to 72 Tg C yr^{-1} . These estimates would imply that atmospheric deposition of fossil carbon accounts for 24 to 41% of fossil OC burial. It should be noted that wet deposition of fossil carbon accounted for 63% of the total atmospheric deposition. The value of $10.8 \text{ Tg C yr}^{-1}$ for fossil OC from wet deposition estimated in this study is comparable to a prior estimate ($12.9 \text{ Tg C yr}^{-1}$) by Zhang et al. (2015a), suggesting that the majority (>80%) of the fossil-derived particulate carbon in wet deposition would be transported to the ocean.

Use of only bulk OC- ^{14}C measurements may overestimate the fossil carbon contributions from river systems discharging to continental margins (Blair and Aller, 2012). Recently, a coupled-isotope ternary mixing model using bulk and compound-specific $\delta^{13}\text{C}$ and $\Delta^{14}\text{C}$ values has been used for apportionment of OC sources in the Yellow River and the BS-YS basin. This approach revealed that pre-aged OC constitutes an important OC component in the Yellow River and BS-YS basin (Tao et al., 2015, 2016; Xue et al., 2017). Similar to marine sedimentary OC, pre-aged OC existing in carbonaceous aerosols (as evidenced by some biomarker proxies; Feng et al., 2007) may overestimate fossil carbon contributions to the CMS. Pre-aged OC in aerosol OC has been indicated by the presence of ^{14}C -depleted plant wax lipids (Eglinton et al., 2002; Matsumoto et al., 2001). For example, the presence of ^{14}C -depleted C_{24-26} long-chain fatty acids (-518‰ , 5860 yr) in a Japan continental aerosol sample suggests long-distance transport from the Asian continent such as the Chinese loess plateau (Matsumoto et al., 2001). Overall, while large uncertainties remain, production and atmospheric deposition of fossil carbon may represent an important source-to-sink term as a component of the OC cycle in the CMS. These and previous estimations underscore the importance of better constraining and integrating atmospheric processes into regional and global ocean carbon cycle studies and models.

5. Conclusions

A wide range in OC $\delta^{13}\text{C}$ (-23.6 to -30.5‰) and $\Delta^{14}\text{C}$ (-153 to -687‰ , 1280 to 9260 ^{14}C age) values of total suspended particles at three coastal sites (CD, QD and HNI) bordering the China marginal seas highlight spatial and temporal variations in carbon sources in terms of biomass and fossil OC contributions. Generally low $\Delta^{14}\text{C}$ values indicate a significant contribution from fossil-fuel emissions to the carbonaceous aerosols, and higher $\delta^{13}\text{C}$ values in winter samples than in summer is attributed to increased coal combustion in winter compared to more petroleum-related emissions in summer.

Quantitative estimates based on ^{14}C mass balance revealed that fossil carbon contributions were high at both the QD (57–64%, ave. = 61%) and HNI (57–67%, ave. = 61%) sites with smaller seasonal variations, implying that both sites were heavily influenced by anthropogenic activity. On the other hand, fossil carbon contribution was lower (26–

73%, ave. = 52%) and exhibited larger seasonal variations at the CD site, reflecting changing contributions from anthropogenic (winter) and biomass (summer) sources.

Fossil carbon input to the CMS through atmospheric deposition ($1.30 \text{ Tg C yr}^{-1}$) was estimated to account for 31% of total fossil carbon input to the CMS, augmenting that from the Yellow River and the Yangtze River ($2.91 \text{ Tg C yr}^{-1}$). Extrapolating this same approach to the global-scale data yields estimates of aerosol fossil carbon input to the global ocean of $17.2 \text{ Tg C yr}^{-1}$, which is equivalent to ~40% of riverine inputs and could account for 24 to 41% of fossil OC burial in marine sediments. Results from both the CMS and global ocean thus suggest that aerosol fossil carbon constitutes an important OC source, and should be integrated into global ocean carbon cycle models.

Acknowledgements

We would like to thank Fengwen Wang and Shixin Guo for sampling help, and Julian Sachs for constructive suggestions and comments on the manuscript. This study was supported by the National Key Research and Development Program of China (Grant No. 2016YFA0601403), and by the National Natural Science Foundation of China (Grant Nos. 41520104009, 41521064), and the “111” Project (B13030). This is MCTL (Key Laboratory of Marine Chemistry Theory and Technology) contribution #152.

Appendix A. Supplementary data

Supplementary data to this article can be found online at <https://doi.org/10.1016/j.scitotenv.2017.11.201>.

References

- Bao, R., McIntyre, C., Zhao, M., Zhu, C., Kao, S.J., Eglinton, T.I., 2016. Widespread dispersal and aging of organic carbon in shallow marginal seas. *Geology* 44, 791–794.
- Blair, N.E., Aller, R.C., 2012. The fate of terrestrial organic carbon in the marine environment. *Annu. Rev. Mar. Sci.* 4, 401–423.
- Blair, N.E., Leithold, E.L., Ford, S.T., Peeler, K.A., Holmes, J.C., Perkey, D.W., 2003. The persistence of memory: the fate of ancient sedimentary organic carbon in a modern sedimentary system. *Geochim. Cosmochim. Acta* 67, 63–73.
- Burdige, D.J., 2005. Burial of terrestrial organic matter in marine sediments: a re-assessment. *Glob. Biogeochem. Cycles* 19, GB4011. <https://doi.org/10.1029/2004GB002368>.
- Cao, J.J., Lee, S.C., Chow, J.C., Watson, J.G., Ho, K.F., Zhang, R.J., Jin, Z.D., Shen, Z.X., Chen, G.C., Kang, Y.M., Zou, S.C., Zhang, L.Z., Qi, S.H., Dai, M.H., Cheng, Y., Hu, K., 2007. Spatial and seasonal distributions of carbonaceous aerosols over China. *J. Geophys. Res.* 112, D22S11. <https://doi.org/10.1029/2006JD008205>.
- Cao, J.J., Chow, J.C., Tao, J., Lee, S.C., Watson, J.G., Ho, K.F., Wang, G.H., Zhu, C.S., Han, Y.M., 2011. Stable carbon isotopes in aerosols from Chinese cities: influence of fossil fuels. *Atmos. Environ.* 45, 1359–1363.
- Chen, B., Andersson, A., Lee, M., Kirillova, E.N., Xiao, Q., Krusa, M., Shi, M., Hu, K., Lu, Z., Streets, D.G., Du, K., Gustafsson, Ö., 2013. Source forensics of black carbon aerosols from China. *Environ. Sci. Technol.* 47, 9102–9108.
- Deng, B., Zhang, J., Wu, Y., 2006. Recent sediment accumulation and carbon burial in the East China Sea. *Glob. Biogeochem. Cycles* 20, GB3014. <https://doi.org/10.1029/2005GB002559>.
- Druffel, E.R., Williams, P.M., Bauer, J.E., Ertel, J.R., 1992. Cycling of dissolved and particulate organic matter in the open ocean. *J. Geophys. Res. Oceans* (1978–2012) 97, 15639–15659.
- Duce, R., Liss, P., Merrill, J., Atlas, E., Buat-Menard, P., Hicks, B., Miller, J., Prospero, J., Arimoto, R., Church, T., 1991. The atmospheric input of trace species to the world ocean. *Glob. Biogeochem. Cycles* 5, 193–259.
- Eglinton, T.I., Eglinton, G., Dupont, L., Montlucon, D., Sholkovitz, E., Reddy, C.M., 2002. Composition, age, provenance of organic matter in N.W. African dust over the Atlantic Ocean. *Geochim. Geophys. Geosyst.* 3, 1–27.
- Fan, Q., Zhang, Y., Ma, W., Ma, H., Feng, J., Yu, Q., Yang, X., Ng, S.K., Fu, Q., Chen, L., 2016. Spatial and seasonal dynamics of ship emissions over the Yangtze River Delta and East China Sea and their potential environmental influence. *Environ. Sci. Technol.* 50, 1322–1329.
- Fang, Y., Chen, Y., Tian, C., Lin, T., Hu, L., Huang, G., Tang, J., Li, J., Zhang, G., 2015. Flux and budget of BC in the continental shelf seas adjacent to Chinese high BC emission source regions. *Glob. Biogeochem. Cycles* 29, 957–972.
- Feng, J., Guo, Z., Chan, C.K., Fang, M., 2007. Properties of organic matter in $\text{PM}_{2.5}$ at Changdao Island, China—a rural site in the transport path of the Asian continental outflow. *Atmos. Environ.* 41, 1924–1935.
- Feng, J.L., Guo, Z.G., Zhang, T.R., Yao, X.H., Chan, C.K., Fang, M., 2012. Source and formation of secondary particulate matter in $\text{PM}_{2.5}$ in Asian continental outflow. *J. Geophys. Res. Atmos.* 117, D03302. <https://doi.org/10.1029/2011JD016400>.
- Fu, H., Chen, J., 2017. Formation, features and controlling strategies of severe haze-fog pollutions in China. *Sci. Total Environ.* 578, 121–138.
- Galy, V., Beyssac, O., France-Lanord, C., Eglinton, T., 2008. Recycling of graphite during Himalayan erosion: a geological stabilization of carbon in the crust. *Science* 322, 943–945.
- Galy, V., Peucker-Ehrenbrink, B., Eglinton, T., 2015. Global carbon export from the terrestrial biosphere controlled by erosion. *Nature* 521, 204–207.
- Guo, Z.G., Sheng, L.F., Feng, J.L., Fang, M., 2003. Seasonal variation of solvent extractable organic compounds in the aerosols in Qingdao, China. *Atmos. Environ.* 37, 1825–1834.
- Gustafsson, Ö., Kruså, M., Zencak, Z., Sheesley, R.J., Granat, L., Engström, E., Praveen, P., Rao, P., Leck, C., Rodhe, H., 2009. Brown clouds over South Asia: biomass or fossil fuel combustion? *Science* 323, 495–498.
- Hanke, U.M., Reddy, C.M., Braun, A.L., Coppola, A., Haghypour, N., McIntyre, C.P., Wacker, L., Xu, L., McNichol, A.P., Abiven, S., Schmidt, M.W., Eglinton, T., 2017. What on Earth have we been burning? Deciphering sedimentary records of pyrogenic carbon. *Environ. Sci. Technol.* <https://doi.org/10.1021/acs.est.7b03243>.
- Heal, M.R., 2014. The application of carbon-14 analyses to the source apportionment of atmospheric carbonaceous particulate matter: a review. *Anal. Bioanal. Chem.* 406, 81–98.
- Hedges, J.L., Keil, R.G., 1995. Sedimentary organic matter preservation: an assessment and speculative synthesis. *Mar. Chem.* 49, 81–115.
- Hu, L.M., Lin, T., Shi, X.F., Yang, Z.S., Wang, H.J., Zhang, G., Guo, Z.G., 2011. The role of shelf mud depositional process and large river inputs on the fate of organochlorine pesticides in sediments of the Yellow and East China seas. *Geophys. Res. Lett.* 38, L03602. <https://doi.org/10.1029/2010GL045723>.
- Hu, B., Li, J., Bi, N., Wang, H., Wei, H., Zhao, J., Xie, L., Zou, L., Cui, R., Li, S., Liu, M., Li, G., 2015. Effect of human-controlled hydrological regime on the source, transport, and flux of particulate organic carbon from the lower Huanghe (Yellow River). *Earth Surf. Process. Landf.* 40, 1029–1042.
- Hu, L., Shi, X., Bai, Y., Qiao, S., Li, L., Yu, Y., Yang, G., Ma, D., Guo, Z., 2016. Recent organic carbon sequestration in the shelf sediments of the Bohai Sea and Yellow Sea, China. *J. Mar. Syst.* 155, 50–58.
- Huang, J., Kang, S., Shen, C., Cong, Z., Liu, K., Wang, W., Liu, L., 2010. Seasonal variations and sources of ambient fossil and biogenic-derived carbonaceous aerosols based on ^{14}C measurements in Lhasa, Tibet. *Atmos. Res.* 96, 553–559.
- Huang, R.J., Zhang, Y., Bozzetti, C., Ho, K.F., Cao, J.J., Han, Y., Daellenbach, K.R., Slowik, J.G., Platt, S.M., Canonaco, F., Zotter, P., Wolf, R., Pieber, S.M., Brunns, E.A., Crippa, M., Ciarelli, G., Piazzalunga, A., Schwikowski, M., Abbaszade, G., Schnelle-Kreis, J., Zimmermann, R., An, Z., Szidat, S., Baltensperger, U., El Haddad, I., Prevot, A.S., 2014. High secondary aerosol contribution to particulate pollution during haze events in China. *Nature* 514, 218–222.
- Huang, L., Zhang, J., Wu, Y., Wang, J., 2016. Distribution and preservation of black carbon in the East China Sea sediments: perspectives on carbon cycling at continental margins. *Deep-Sea Res. II* 124, 43–52.
- Jurado, E., Dachs, J., Duarte, C.M., Simó, R., 2008. Atmospheric deposition of organic and black carbon to the global oceans. *Atmos. Environ.* 42, 7931–7939.
- Klinedinst, D.B., Currie, L.A., 1999. Direct quantification of $\text{PM}_{2.5}$ fossil and biomass carbon within the Northern Front Range Air Quality Study's domain. *Environ. Sci. Technol.* 33, 4146–4154.
- Lamb, A.L., Wilson, G.P., Leng, M.J., 2006. A review of coastal palaeoclimate and relative sea-level reconstructions using $\delta^{13}\text{C}$ and C/N ratios in organic material. *Earth-Sci. Rev.* 75, 29–57.
- Levin, I., Kromer, B., Schmidt, M., Sartorius, H., 2003. A novel approach for independent budgeting of fossil fuel CO_2 over Europe by ^{14}C observations. *Geophys. Res. Lett.* 30 (23):2194. <https://doi.org/10.1029/2003GL018477>.
- Lin, T., Hu, L., Guo, Z., Qin, Y., Yang, Z., Zhang, G., Zheng, M., 2011. Sources of polycyclic aromatic hydrocarbons to sediments of the Bohai and Yellow Seas in East Asia. *J. Geophys. Res. Atmos.* 116, D23305. <https://doi.org/10.1029/2011JD015722>.
- Liu, D., Li, J., Zhang, Y., Xu, Y., Liu, X., Ding, P., Shen, C., Chen, Y., Tian, C., Zhang, G., 2013. The use of levoglucosan and radiocarbon for source apportionment of $\text{PM}_{2.5}$ carbonaceous aerosols at a background site in East China. *Environ. Sci. Technol.* 47, 10454–10461.
- Mahowald, N., 2011. Aerosol indirect effect on biogeochemical cycles and climate. *Science* 334, 794–796.
- Mandalakis, M., Gustafsson, Ö., Alsberg, T., Egeback, A.-L., Reddy, C.M., Xu, L., Klanova, J., Holoubek, I., Stephanou, E.G., 2005. Contribution of biomass burning to atmospheric polycyclic aromatic hydrocarbons at three European background sites. *Environ. Sci. Technol.* 39, 2976–2982.
- Matsumoto, K., Kawamura, K., Uchida, M., Shibata, Y., Yoneda, M., 2001. Compound specific radiocarbon and $\delta^{13}\text{C}$ measurements of fatty acids in a continental aerosol sample. *Geophys. Res. Lett.* 28, 4587–4590.
- McNichol, A.P., Schneider, R.J., Von Reden, K.F., Gagnon, A.R., Elder, K.L., Key, R.M., Quay, P.D., 2000. Ten years after—the WOCE AMS radiocarbon program. *Nucl. Inst. Methods Phys. Res. B* 172, 479–484.
- Shang, D., Hu, M., Guo, Q., Zou, Q., Zheng, J., Guo, S., 2017. Effects of continental anthropogenic sources on organic aerosols in the coastal atmosphere of East China. *Environ. Pollut.* 229, 350–361.
- Sheesley, R.J., Kirillova, E., Andersson, A., Kruså, M., Praveen, P.S., Budhavant, K., Safai, P.D., Rao, P.S.P., Gustafsson, Ö., 2012. Year-round radiocarbon-based source apportionment of carbonaceous aerosols at two background sites in South Asia. *J. Geophys. Res. Atmos.* 117, D10202. <https://doi.org/10.1029/2011JD017161>.
- Stuiver, M., Polach, H.A., 1977. Discussion; reporting of ^{14}C data. *Radiocarbon* 19, 355–363.
- Sun, X., Hu, M., Guo, S., Liu, K., Zhou, L., 2012. ^{14}C -based source assessment of carbonaceous aerosols at a rural site. *Atmos. Environ.* 50, 36–40.

- Tao, S., Eglinton, T.I., Montluçon, D.B., McIntyre, C., Zhao, M., 2015. Pre-aged soil organic carbon as a major component of the Yellow River suspended load: regional significance and global relevance. *Earth Planet. Sci. Lett.* 414, 77–86.
- Tao, S., Eglinton, T.I., Montluçon, D.B., McIntyre, C., Zhao, M., 2016. Diverse origins and pre-depositional histories of organic matter in contemporary Chinese marginal sea sediments. *Geochim. Cosmochim. Acta* 191, 70–88.
- Uchida, M., Kumata, H., Koike, Y., Tsuzuki, M., Uchida, T., Fujiwara, K., Shibata, Y., 2010. Radiocarbon-based source apportionment of black carbon (BC) in PM 10 aerosols from residential area of suburban Tokyo. *Nucl. Inst. Methods Phys. Res. B* 268, 1120–1124.
- Wang, X., Ma, H., Li, R., Song, Z., Wu, J., 2012. Seasonal fluxes and source variation of organic carbon transported by two major Chinese Rivers: the Yellow River and Changjiang (Yangtze) River. *Glob. Biogeochem. Cycles* 26, GB2025. <https://doi.org/10.1029/2011GB004130>.
- Wang, F., Guo, Z., Lin, T., Hu, L., Chen, Y., Zhu, Y., 2015a. Characterization of carbonaceous aerosols over the East China Sea: the impact of the East Asian continental outflow. *Atmos. Environ.* 110, 163–173.
- Wang, Q., Zhuang, G., Huang, K., Liu, T., Deng, C., Xu, J., Lin, Y., Guo, Z., Chen, Y., Fu, Q., Fu, J.S., Chen, J., 2015b. Probing the severe haze pollution in three typical regions of China: characteristics, sources and regional impacts. *Atmos. Environ.* 120, 76–88.
- Wang, F., Chen, Y., Meng, X., Fu, J., Wang, B., 2016a. The contribution of anthropogenic sources to the aerosols over East China Sea. *Atmos. Environ.* 127, 22–33.
- Wang, X., Ge, T., Xu, C., Xue, Y., Luo, C., 2016b. Carbon isotopic (^{14}C and ^{13}C) characterization of fossil-fuel derived dissolved organic carbon in wet precipitation in Shandong Province, China. *J. Atmos. Chem.* 73, 207–221.
- Wang, C., Zou, X., Zhao, Y., Li, Y., Song, Q., Wang, T., Yu, W., 2017a. Distribution pattern and mass budget of sedimentary polycyclic aromatic hydrocarbons in shelf areas of the Eastern China Marginal Seas. *J. Geophys. Res. Oceans* 112, 4990–5004.
- Wang, F.J., Chen, Y., Guo, Z.G., Gao, H.W., Mackey, K.R., Yao, X.H., Zhuang, G.S., Paytan, A., 2017b. Combined effects of iron and copper from atmospheric dry deposition on ocean productivity. *Geophys. Res. Lett.* 44, 2546–2555.
- Willey, J.D., Kieber, R.J., Eyman, M.S., Avery, G.B., 2000. Rainwater dissolved organic carbon: concentrations and global flux. *Glob. Biogeochem. Cycles* 14, 139–148.
- Wu, Y., Eglinton, T., Yang, L., Deng, B., Montluçon, D., Zhang, J., 2013. Spatial variability in the abundance, composition, and age of organic matter in surficial sediments of the East China Sea. *J. Geophys. Res. Biogeosci.* 118, 1495–1507.
- Xing, L., Zhao, M., Gao, W., Wang, F., Zhang, H., Li, L., Liu, J., Liu, Y., 2014. Multiple proxy estimates of source and spatial variation in organic matter in surface sediments from the southern Yellow Sea. *Org. Geochem.* 76, 72–81.
- Xing, L., Hou, D., Wang, X., Li, L., Zhao, M., 2016. Assessment of the sources of sedimentary organic matter in the Bohai Sea and the northern Yellow Sea using biomarker proxies. *Estuar. Coast. Shelf Sci.* 176, 67–75.
- Xue, Y., Zou, L., Ge, T., Wang, X., 2017. Mobilization and export of millennial-aged organic carbon by the Yellow River. *Limnol. Oceanogr.* <https://doi.org/10.1002/lno.10579>.
- Yoon, S.H., Kim, J.H., Yi, H.I., Yamamoto, M., Gal, J.K., Kang, S., Shin, K.H., 2016. Source, composition and reactivity of sedimentary organic carbon in the river-dominated marginal seas: a study of the eastern Yellow Sea (the northwestern Pacific). *Cont. Shelf Res.* 125, 114–126.
- Zencak, Z., Klanova, J., Holoubek, I., Gustafsson, Ö., 2007. Source apportionment of atmospheric PAHs in the western Balkans by natural abundance radiocarbon analysis. *Environ. Sci. Technol.* 41, 3850–3855.
- Zhang, Y.L., Li, J., Zhang, G., Zotter, P., Huang, R.J., Tang, J.H., Wacker, L., Prevot, A.S., Szidat, S., 2014. Radiocarbon-based source apportionment of carbonaceous aerosols at a regional background site on Hainan Island, South China. *Environ. Sci. Technol.* 48, 2651–2659.
- Zhang, Y.L., Cerqueira, M., Salazar, G., Zotter, P., Hueglin, C., Zellweger, C., Pio, C., Prévôt, A.S.H., Szidat, S., 2015a. Wet deposition of fossil and non-fossil derived particulate carbon: insights from radiocarbon measurement. *Atmos. Environ.* 115, 257–262.
- Zhang, Y.L., Huang, R.J., El Haddad, I., Ho, K.F., Cao, J.J., Han, Y., Zotter, P., Bozzetti, C., Daellenbach, K.R., Canonaco, F., Slowik, J.G., Salazar, G., Schwikowski, M., Schnelle-Kreis, J., Abbazade, G., Zimmermann, R., Baltensperger, U., Prévôt, A.S.H., Szidat, S., 2015b. Fossil vs. non-fossil sources of fine carbonaceous aerosols in four Chinese cities during the extreme winter haze episode of 2013. *Atmos. Chem. Phys.* 15, 1299–1312.
- Zhang, Y., Ren, H., Sun, Y., Cao, F., Chang, Y., Liu, S., Lee, X., Agrios, K., Kawamura, K., Liu, D., Ren, L., Du, W., Wang, Z., Prevot, A.S.H., Szidat, S., Fu, P., 2017. High contribution of nonfossil sources to submicrometer organic aerosols in Beijing, China. *Environ. Sci. Technol.* 51, 7842–7852.
- Zhou, L., Liu, J., Saito, Y., Zhang, Z., Chu, H., Hu, G., 2014. Coastal erosion as a major sediment supplier to continental shelves: example from the abandoned Old Huanghe (Yellow River) delta. *Cont. Shelf Res.* 82, 43–59.